

Sub-Poissonian atomic statistics in a micromaser

Gerhard Rempe and Herbert Walther

*Sektion Physik der Universität München and Max-Planck-Institut für Quantenoptik,
D-8046 Garching bei München, West Germany*

(Received 7 February 1990)

It is shown analytically that under certain experimental conditions the steady-state photon statistics of a micromaser field are directly connected to the fluctuation in number of the atoms in transition from the upper to the lower maser level under the influence of the maser field. The analytical results are compared to the results of a computer simulation of the maser process.

I. INTRODUCTION

In recent years, it has been demonstrated that maser action can be achieved with, on average, less than a single excited atom in a superconducting microwave cavity.^{1,2} This one-atom maser or micromaser is operated with Rydberg atoms, i.e., atoms with a valence electron in a highly excited orbit having extremely large dipole moments for transitions to neighboring levels. The micromaser fulfills, in a perfect way, the idealized conditions treated by Jaynes and Cummings in the pioneer days of masers and lasers:³ one single atom interacting with a single mode of the cavity field. Owing to the large atom-field coupling for Rydberg atoms, the atoms can exchange photons with the field several times while they travel through the cavity. Since the velocity of the atoms can be preselected, e.g., by using a Fizeau-type velocity selector,² the interaction time can be fixed, which leads to conditions usually not achievable in standard masers: the field produced in the cavity shows nonclassical properties, i.e., the number distribution of the photons in the cavity can be sub-Poissonian.^{4,5} It has been shown that even a number state can be generated using a cavity with a high enough quality factor and with no thermal photons in the cavity to begin with.^{6,7} Both conditions can be fulfilled when the superconducting cavity is operated at very low temperatures, e.g., <0.5 K. In this case more interesting features may show up, such as trapping states of the cavity.⁸

It turns out that the measurement of the nonclassical photon statistics in the cavity is not that easy. In order to measure the field it has to be coupled to a measuring device whereby losses are introduced leading to a destruction of the nonclassical properties. The best method to investigate the field is to use the Rydberg atoms themselves. One way is to measure the statistics via the dynamical behavior of the atoms in the radiation field by studying the collapse and the revivals.^{2,9} However, it is much better and more conclusive to probe the population of the atoms in the upper and lower maser levels after they have left the cavity. In this case, the interaction time is kept constant.² This is an advantage since the steady-state photon-number distribution changes with the interaction time. The measurement of the atom num-

ber fluctuations is relatively easy since electric fields can be used to perform a selective ionization of the atoms. The detection sensitivity is sufficient so that the atomic statistics can be investigated.

This paper is organized as follows. In Sec. II, we will analytically derive a connection between atom statistics and field statistics. This formula allows us to evaluate ongoing experiments with our micromaser. We assume that the measurements are performed in a regime where the counting interval for the atoms is larger or identical to the cavity decay time. Furthermore, it is assumed that the maser is operating under steady-state conditions. The parameters that the calculations are based upon are identical to the ones used in our experiments.¹⁰ In Sec. III, the analytical formula is tested by a numerical simulation of the maser process. In addition, the dependence of the atom statistics upon both the counting time interval and the detection efficiency are studied. Section IV is a short summary and conclusion.

II. ANALYTICAL CALCULATION

The probability of finding a single atom in the lower maser level is given by³

$$P = \sum_{n=0}^{\infty} p_n \sin^2[\Omega t_{\text{int}}(n+1)^{1/2}], \quad (1)$$

where p_n describes the probability distribution for the photons, Ω the atom-field coupling constant, and t_{int} the interaction time of the atom with the cavity field. As soon as the steady state is reached, the photon-number distribution, on average, does not change any more between successive atoms. The photon-number distribution is given by^{4,5}

$$p_n = C(N_{\text{ex}}) \prod_{k=1}^n \frac{N_{\text{ex}} \sin^2(\Omega t_{\text{int}} k^{1/2})}{k}, \quad (2)$$

where N_{ex} stands for the number of atoms passing through the cavity in the decay time T_{cav} of the radiation field, and $C(N_{\text{ex}})$ is a normalization constant depending on N_{ex} . In deriving Eq. (2) for the photon statistics, it is assumed that the atoms entering the cavity obey Poisson statistics. Furthermore, thermal photons are neglected in

Eq. (2). This is justified for our present experiment operated at a cavity temperature of 0.5 K and a frequency of 21.5 GHz, which leads to a mean number of thermal photons in the cavity of about 0.15. Also, the flux is small so that there is never more than a single atom in the cavity.

In the following, we consider a measurement time interval T identical to T_{cav} and use $N = N_{\text{ex}}$, dropping the index for simplicity. For measurement intervals $T > T_{\text{cav}}$, the connection between N and N_{ex} is given by $N_{\text{ex}} = NT_{\text{cav}}/T$, so that the limitation $T = T_{\text{cav}}$ used in this paper is not an essential restriction. The only restriction for the time interval results from the fact that we require the steady state of the photon distribution. For a fixed number of atoms N entering the cavity in the upper maser level, the probability of finding m atoms in the lower state after they passed through the cavity is then given by a binomial distribution $B_m(N)$

$$B_m(N) = \binom{N}{m} P(N)^m [1 - P(N)]^{N-m} \quad (3)$$

with a mean $\langle m \rangle = NP(N)$ and a variance

$$\langle m^2 \rangle - \langle m \rangle^2 = NP(N)[1 - P(N)].$$

However, the number of atoms N observed in the time interval T will fluctuate due to the Poissonian statistics of the atomic beam. This fact has to be taken into account. We will do so in the following. In the case of the steady state, the influence of the fluctuations of N on the probability $P(N)$ therefore only enters via the atomic flux. In order to calculate the variation of P , the number of atoms N is considered a variable.

As mentioned already, the variation of N obeys Poissonian statistics which will be introduced by the probability distribution p_N . The binomial distribution $B_m(N)$ has to be combined with p_N in order to obtain the probability W_m of finding m atoms in the lower state

$$W_m = \sum_{N=0}^{\infty} p_N B_m(N). \quad (4)$$

We now calculate the mean number of atoms in the lower level $\langle m \rangle$ and the variance $\langle m^2 \rangle - \langle m \rangle^2$ using W_m :

$$\begin{aligned} \langle m \rangle &= \sum_{m=0}^{\infty} m W_m = \sum_{m=0}^{\infty} m \sum_{N=0}^{\infty} p_N B_m(N) \\ &= \sum_{N=0}^{\infty} p_N NP(N). \end{aligned} \quad (5)$$

As $P(N)$ is slowly varying with N , we can expand $P(N)$ in the vicinity of $\langle N \rangle$. We obtain

$$P(N) = P(\langle N \rangle) + (N - \langle N \rangle) dP/dN + \dots \quad (6)$$

The lowest-order term gives

$$\langle m \rangle = \langle N \rangle P(\langle N \rangle) + \langle N \rangle dP/dN, \quad (7)$$

where we have used $\langle N^2 \rangle - \langle N \rangle^2 = \langle N \rangle$ for the atoms entering the cavity. This is valid for a Poisson process. The derivative dP/dN has to be calculated at the value

$N = \langle N \rangle$. It is evident from the result (7) that the mean number of atoms in the lower state $\langle m \rangle$ is changing because P depends on the flux of atoms N . In the same way we obtain

$$\begin{aligned} \langle m^2 \rangle &= \sum_{m=0}^{\infty} m^2 W_m \\ &= \sum_{N=0}^{\infty} p_N [NP(N) + (N^2 - N)P(N)^2]. \end{aligned} \quad (8)$$

Inserting the expansion of $P(N)$ from Eq. (6) into expression (8), we get the result

$$\begin{aligned} \langle m^2 \rangle &= P(\langle N \rangle) \langle N \rangle + P(\langle N \rangle)^2 \langle N \rangle^2 \\ &\quad + [\langle N \rangle + 4P(\langle N \rangle) \langle N \rangle^2] dP/dN \\ &\quad + [\langle N \rangle^3 + 4\langle N \rangle^2] (dP/dN)^2. \end{aligned} \quad (9)$$

We now define the normalized variance of the atoms in the lower state Q_a . This definition is analogous to the one introduced by Mandel for photon statistics:¹¹

$$Q_a = \frac{\langle m^2 \rangle - \langle m \rangle^2}{\langle m \rangle} - 1. \quad (10)$$

Inserting the results for $\langle m \rangle$ and $\langle m^2 \rangle$ from Eqs. (7) and (9), respectively, into definition (10) we obtain for $\langle N \rangle \gg 1$,

$$Q_a = \frac{2P(\langle N \rangle) \langle N \rangle dP/dN + \langle N \rangle^2 (dP/dN)^2}{P(\langle N \rangle)}. \quad (11)$$

This formula is a general result which will be used to calculate the normalized variance of the atoms leaving the cavity in the lower level. Higher-order terms have been neglected. It is obvious that $dP/dN = 0$ implies $Q_a = 0$, which means that a constant fraction P of the atoms leaves the cavity in the lower state; the atoms do not influence each other, so that we have an ideal Poisson process. If $dP/dN \neq 0$ and is negative, this leads to a situation where an increasing number of atoms N crossing the cavity gives rise to a decreasing probability of finding atoms in the lower state and vice versa. This mechanism counterbalances the flux of atoms in the lower state and thus stabilizes the number of atoms leaving the cavity in the lower state. The consequence is a sub-Poissonian distribution. We show below [see the discussion following Eqs. (19) and (20)] that, in this situation, the second term in Eq. (11) for the normalized atomic variance is dominated by the first term which is negative. Therefore, it follows from Eq. (11) that $Q_a < 0$. Of course, for positive dP/dN , we expect a super-Poissonian distribution with $Q_a > 0$. In this case, both terms in Eq. (11) are positive.

We want to emphasize that the reason for the sub-Poissonian atomic statistics is the following: a changing flux of atoms changes the Rabi frequency via the stored photon number in the cavity. By adjusting the interaction time, the phase of the Rabi nutation cycle can be chosen such that the probability for the atoms leaving the cavity in the upper maser level is increasing when the flux, and therefore the photon number, is enlarged or vice versa. We expect sub-Poissonian atomic statistics in the case where dP/dN is negative, i.e., when the number of

atoms in the lower state is decreasing with increasing flux and photon number in the cavity.

In Sec. III, we derive the connection between the atomic variance Q_a and the normalized variance Q_f of the photons in the cavity. Q_f is defined similarly to Q_a , however, the number of atoms m has to be replaced by the number of photons n . As can be seen from Eq. (11), we need the derivative dP/dN for calculating Q_a . According to Eq. (1), the probability P of finding an atom in the lower level is determined by the photon-number distribution p_n which is given by Eq. (2). We obtain

$$\frac{dp_n}{dN} = \frac{n - \langle n \rangle}{\langle N \rangle} p_n. \quad (12)$$

[Note that the normalization constant $C(N)$ depends on N .] Therefore, dP/dN is given by the formula

$$\frac{dP}{dN} = \sum_{n=0}^{\infty} \frac{n - \langle n \rangle}{\langle N \rangle} p_n \sin^2[\Omega t_{\text{int}}(n+1)^{1/2}]. \quad (13)$$

Using the micromaser photon statistics p_n from (2), we see that

$$\frac{dP}{dN} = \sum_{n=0}^{\infty} \frac{n - \langle n \rangle}{\langle N \rangle} p_{n+1} \frac{n+1}{\langle N \rangle}, \quad (14)$$

or if we change the summation index from $n+1$ to n , we get

$$\frac{dP}{dN} = \frac{1}{\langle N \rangle^2} \sum_{n=1}^{\infty} (n^2 - n - n \langle n \rangle) p_n \quad (15)$$

$$= \frac{1}{\langle N \rangle^2} \sum_{n=0}^{\infty} (n^2 - n - n \langle n \rangle) p_n. \quad (16)$$

This gives

$$\frac{dP}{dN} = \frac{\langle n \rangle}{\langle N \rangle^2} Q_f. \quad (17)$$

Analogous to the derivation of Eq. (17), it is easy to show that the mean photon number is given by

$$\langle n \rangle = P(\langle N \rangle) \langle N \rangle, \quad (18)$$

as expected by energy conservation. Combining these two equations, i.e., (17) and (18), it is straightforward to verify that

$$2P(\langle N \rangle) \langle N \rangle \frac{dP}{dN} = P(\langle N \rangle)^2 2Q_f \quad (19)$$

and

$$\langle N \rangle^2 \left[\frac{dP}{dN} \right]^2 = P(\langle N \rangle)^2 Q_f^2. \quad (20)$$

As can be seen, the two terms in Eq. (11) for the atomic variance Q_a can be calculated with the help of formulas (19) and (20), respectively. For negative dP/dN , and therefore negative $0 > Q_f \geq -1$, i.e., $|2Q_f| > Q_f^2$, we have thus shown that the first term in Eq. (11) determines the sign of Q_a . It follows that the negative value of dP/dN is responsible for the sub-Poissonian statistics of the photon field. This feature is special for the micromaser and not

shared by usual lasers or masers.

Inserting the last two equations, (19) and (20), into Eq. (11) for the atomic variance, we obtain the variance equation

$$Q_a = P(\langle N \rangle) Q_f (2 + Q_f), \quad (21)$$

which gives us the normalized variance of the atoms Q_a in terms of Q_f of the field. It is independent of the measuring time T . In deriving formula (21), we have neglected all terms proportional to $1/\langle N \rangle$. This variance equation (21) is the central result of our calculation. It is valid for times T longer than or equal to the decay time of the maser field and a temperature low enough in order to neglect the thermal photons. It shows that the atomic statistics are closely related to the statistics of the maser field. In particular, the sub-Poissonian photon statistics can be measured via the atomic statistics which are then also sub-Poissonian. A maser field with reduced photon-number fluctuations generates a stable flux of atoms in the lower level.

Figure 1 shows Q_a as a function of the dimensionless maser pump parameter $\theta = \Omega t_{\text{int}} \langle N \rangle^{1/2}$ for $\langle N \rangle = N_{\text{ex}} = 20$. The variance equation (21) was used for plotting the solid line. The photon statistics were calculated from the micromaser theory.^{4,5} In addition, a detection efficiency of 0.1 typical for the experiment¹⁰ was taken into account by multiplying the values derived from the variance equation (21) by a factor of 0.1. This is justified in the case of a random deletion. It should also be mentioned that 0.1 blackbody photons per cavity mode were assumed in order to prevent trapping states⁸ from show-

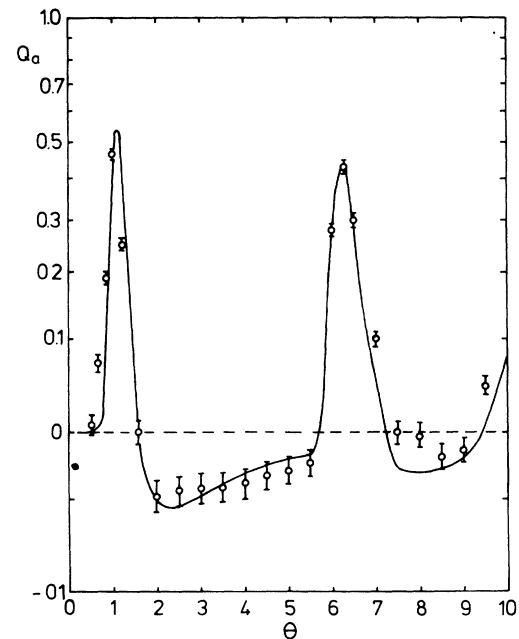


FIG. 1. Comparison between the result of the variance equation (21) and the computer simulation. The normalized atomic variance Q_a defined in Eq. (10) is plotted as a function of the dimensionless maser pump parameter θ for $N_{\text{ex}} = 20$ and $n_b = 0.1$.

ing up in the figure. [The thermal photons are considered for calculating Q_f , which is needed for the evaluation of Q_a using (21).] As is displayed, the atomic variance Q_a shows two maxima corresponding to increased photon-number fluctuations in the micromaser cavity. They are due to phase transitions where the mean photon number increases abruptly as a function of θ . This feature is unique for the micromaser with a well-defined atom-field interaction time; the large fluctuations of the mean photon number known from micromaser theory result in equivalent fluctuations of the number of atoms leaving the cavity in the lower state. In the regions between the maxima, the normalized variance of the photon statistics Q_f and also of the atomic statistics Q_a are negative corresponding to sub-Poissonian fluctuations.

III. NUMERICAL SIMULATION

In order to test the validity of the assumptions made in deriving the variance equation (21), a numerical simulation of the maser process has been performed. This was done following the procedure used by Meystre and Wright¹² who were interested in the photon statistics of the micromaser. We, in addition, extend the calculations in order to obtain the statistics of the atoms leaving the cavity.

In the simulation, the successive passages of atoms through the maser cavity are explicitly taken into account. Atoms are injected into the cavity one at a time and exposed to the cavity field with the photon statistics $p_n(t)$. When they leave the resonator, they are found to be either in the lower or the upper maser level. In the previous simulations,¹² it was assumed that the detection efficiency was $\epsilon=1$. In contrast to that, we assume here a more realistic value of $\epsilon=0.1$. The determination of the photon number in the cavity depends on whether an atom is detected or not. In the computer program, this effect is taken into account by using a random number generator for the interval $[0,1]$. If the number is larger than 0.1, the atom is treated as not detected and the photon statistics change according to

$$p_n(t+t_{\text{int}}) = p_n(t)\cos^2[\Omega t_{\text{int}}(n+1)^{1/2}] + p_{n-1}(t)\sin^2(\Omega t_{\text{int}}n^{1/2}). \quad (22)$$

Otherwise, the atom is treated as detected and a new random number serves to simulate the outcome of the measurement. This is done by comparing the new random number with the Jaynes-Cummings probability of finding the atom in the lower maser level, which is given by Eq. (1). If the number is larger than the Jaynes-Cummings probability, then the atom is taken to be in the upper state, if it smaller, the atom is assumed to be in the lower state. After the interaction, the photon statistics in the cavity depend upon the state of the atom and are given either by

$$p_n(t+t_{\text{int}}) = \mathcal{N}_\downarrow p_{n-1}(t)\sin^2(\Omega t_{\text{int}}n^{1/2}) \quad (23)$$

for atoms in the lower level or by

$$p_n(t+t_{\text{int}}) = \mathcal{N}_\uparrow p_n(t)\cos^2[\Omega t_{\text{int}}(n+1)^{1/2}] \quad (24)$$

for atoms in the upper level. Here, \mathcal{N}_\downarrow and \mathcal{N}_\uparrow are two normalization constants. During the intervals between successive atoms, the evolution of the cavity field is treated using the master equation of a damped harmonic oscillator interacting with a thermal bath with a mean number of $n_b=0.1$ blackbody photons. This corresponds to the cavity temperature used in the experiments.⁹ The photon statistics change according to

$$T_{\text{cav}} \frac{dp_n}{dt} = (n_b+1)[(n+1)p_{n+1} - np_n] + n_b[np_{n-1} - (n+1)p_n]. \quad (25)$$

The spacing of the atoms obeys Poissonian statistics. The total sampling time interval is taken to be two cavity decay times; this ensures steady-state conditions. From the fluctuations of the number of atoms in the lower state, the variance Q_a of the atoms is finally determined.

Results of the simulation are given by the circles in Fig. 1. For each data point, about 1 000 000 atoms at a rate of $N_{\text{ex}}=20$ were used for the calculation corresponding to 25 000 sampling time intervals which were averaged. In this way, the error of the numerical calculation is kept on the order of 1%. The agreement between the numerical simulation and the result obtained by using the variance equation (21) is good, as can be seen in Fig. 1. The small deviation near $\theta=8$ can be traced back to the existence of a trapping state,⁸ which still remains present even for 0.1 blackbody photons in the cavity. This effect does not show up in the solid line since there, the trapping states are washed out already at smaller blackbody photon numbers. This phenomenon is due to the fact that the ensemble average, which is the basis of the micromaser theory, differs from the result of the numerical simulation; details of this difference will be worked out in the following.

The physical mechanism responsible for the sub-Poissonian atomic statistics is the backcoupling of the cavity field on the atomic population in the lower level. This leads to a reduction of the number fluctuations. The time constant for this feedback mechanism is the decay time of the cavity field T_{cav} . Therefore, fluctuations on a time scale short compared to T_{cav} are not suppressed in the maser. This is confirmed by Fig. 2, where the normalized atomic variance Q_a is plotted as a function of the sampling time interval T for $\theta=5$, $N_{\text{ex}}=35$, and $n_b=0.1$. Two different detection efficiencies of $\epsilon=0.1$ and 1.0 are considered. Results of the simulation are represented by crosses and circles, respectively. It is obvious from Fig. 2 that Q_a does not depend on T for measurement time intervals larger than the cavity decay time. This justifies the assumption $T=T_{\text{cav}}$ made above in the derivation of the variance equation (21).

As can be seen from Fig. 2, the magnitude of the non-classical character, i.e., $Q_a < 0$, is reduced in the simulation with $\epsilon=0.1$ as compared to $\epsilon=1.0$. Under the action of a random deletion, the measured atom statistics move toward the Poisson distribution as the limiting case. It has been shown under general conditions¹³ that the normalized variance of a point process undergoing random deletion is proportional to the deletion parameter

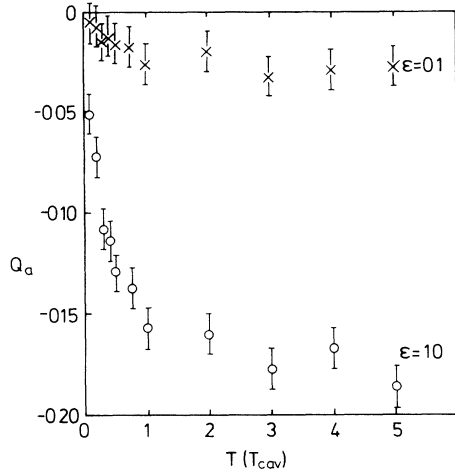


FIG. 2. Normalized atomic variance Q_a plotted as a function of the sampling time interval T for $N_{\text{ex}}=35$, $\theta=5$, and $n_b=0.1$. Time is given in units of T_{cav} .

which is given by the detection efficiency in our simulation. The results plotted in Fig. 2, however, show that this proportionality is not true in the present situation. Here, a detection efficiency below unity influences the photon statistics in the cavity according to Eq. (22) if the atom is not detected and according to Eqs. (23) or (24) if the atom is detected in the lower or upper level, respectively. Therefore, depending on the outcome of a measurement, the photon statistics change in a different manner and the detection efficiency does not show up as a Bernoulli random deletion process. It follows that the normalized variance Q_a is not proportional to the detection efficiency ϵ . In particular (see Fig. 2), when ϵ is increased by a factor of 10, the magnitude of Q_a increases by a factor of only 6–7.

For a detection sensitivity of $\epsilon=1.0$, the measurement process reduces the nonclassical effect $Q_a > 0$. This reduction can be understood from the following discussion: Starting from the micromaser photon statistics at time t as given in Eq. (2) with a mean photon number $\langle n(t) \rangle$ and using Eq. (23), it is easy to show that the detection of an atom in the lower maser level changes the photon statistics according to

$$p_n(t+t_{\text{int}}) = \mathcal{N}_\downarrow p_n(t) n / N_{\text{ex}} . \quad (26)$$

From this, the mean number of photons after the interaction can be calculated:

$$\langle n(t+t_{\text{int}}) \rangle_\downarrow = \langle n(t) \rangle + Q_f + 1 . \quad (27)$$

This equation leads to the interesting conclusion that $\langle n \rangle$ only increases by one if the normalized variance Q_f of the photon-number distribution vanishes. For negative (positive) Q_f , the mean photon number increases by less (more) than one despite the fact that the atom made a transition from the upper to the lower maser level thereby emitting one photon. This phenomenon does not violate energy conservation because $\langle n(t) \rangle$ is known only to within its standard deviation $Q_f + 1$. For $Q_f = -1$, all atoms leave the cavity in the excited state

($P=0$) and Eq. (27) becomes meaningless.

The damping of the maser field in the time interval t_a between successive atoms is taken into account by multiplying Eq. (27) for the mean photon number with the factor $N_{\text{ex}} \gg 1$

$$\exp(-t_a/T_{\text{cav}}) \approx \exp(-1/N_{\text{ex}}) \approx 1 - 1/N_{\text{ex}} . \quad (28)$$

The mean photon number of the maser field when the next atom enters the cavity has therefore changed according to

$$\langle n(t) \rangle \rightarrow \langle n(t+t_{\text{int}}+t_a) \rangle_\downarrow = \langle n(t) \rangle + Q_f + 1 - P . \quad (29)$$

Equation (18) was used for the probability P of finding the atom in the lower level. A similar calculation leads to the result

$$\langle n(t) \rangle \rightarrow \langle n(t+t_{\text{int}}+t_a) \rangle_\uparrow = \langle n(t) \rangle - \frac{Q_f P}{1-P} - P \quad (30)$$

if the first atom is detected in the upper state. A measurement of the atom which is not state selective does not change the mean number of maser photons. This steady-state condition is used in Ref. 4 to derive the micromaser photon statistics given by Eq. (2).

If an atom is detected in the lower level, Eq. (29) implies that, for a nonclassical field with $Q_f < P - 1 < 0$, the mean number of photons decreases from this atom to the next. As discussed in Sec. II, a similar, but larger, effect is caused by a decreasing atomic flux. The smaller intensity of the field which causes a lower Rabi frequency therefore increases the probability of finding the following atom in the lower state as well. Hence, this measurement-induced effect leads to a bunching of atoms in the lower level and decreases the magnitude of the nonclassical normalized variance Q_a of atoms in the case of a high-detection sensitivity. Under the same condition, i.e., $Q_f < P - 1 < 0$, it follows from Eq. (30) that the mean photon number as seen by the second atom increases if the first atom is measured in the upper state. The enlarged Rabi frequency then leads to a similar bunching of atoms in the upper state.

This bunching effect is not restricted to the condition $Q_f < P - 1$, which can easily be realized in the micromaser but is present even for large photon-number fluctuations with $Q_f > 0$. According to Eq. (29), a detection of an atom in the lower level, in this case, implies an increase in the mean number of photons with a correspondingly enlarged Rabi frequency. As discussed in Sec. II, for $Q_f > 0$ and therefore $Q_a > 0$, the higher intensity of the field leads to a higher probability of finding the next atom in the lower state as well.

For a small detection efficiency, this bunching phenomenon disappears because Eq. (22) is predominantly used and the fluctuations introduced by the measurement process are averaged out. With increasing detection efficiency, the cavity field is disturbed by the measurement process as expressed by Eqs. (23) and (24) or (29) and (30). State selective measurements of the atoms decrease the width of the actual photon-number distribution but prevent the micromaser field from reaching a

unique steady state. The distribution given by Eq. (2) is obtained when the photon statistics are averaged over many atoms. It follows that the nonclassical character of the normalized variance Q_a of atoms in the lower level is decreased in magnitude in the case of a high-detection efficiency near unity: Q_a depends less than linearly on the detection efficiency. The measurement process generally increases the fluctuations of the mean photon number and the number of atoms detected: this is not unexpected since the micromaser is a quantum system. The measurement process must therefore influence the result.

IV. CONCLUSIONS

To sum up, we have derived the connection between the photon statistics in the micromaser cavity and the atomic statistics of the atoms in the lower state after they passed through the cavity. It is straightforward to determine the photon statistics from the variance equation (21) under the special conditions we discussed above. This

situation corresponds to the conditions of our present micromaser experiment. The quality factor of the micromaser cavity used is 3×10^{10} . At a frequency of 21.5 GHz, this corresponds to a decay time of the field of 200 ms. The atoms cross the cavity in about 100 μ s. Therefore, it is possible to have several hundred atoms entering the cavity within the decay time; nevertheless, the average time interval between the atoms is long enough so that the single-atom condition is maintained. Experiments to measure the photon statistics via the statistics of the atoms as discussed above have been performed recently and will be published elsewhere.¹⁰

ACKNOWLEDGMENTS

The authors would like to thank M. O. Scully, P. Meystre, A. Schenzle, and W. Schleich for many valuable discussions. A part of the computer simulations were performed by C. Weinmann; the authors would like to thank her for this valuable help.

-
- ¹D. Meschede, H. Walther, and G. Müller, *Phys. Rev. Lett.* **54**, 551 (1985).
²G. Rempe, H. Walther, and N. Klein, *Phys. Rev. Lett.* **58**, 353 (1987).
³E. T. Jaynes and F. W. Cummings, *Proc. IEEE* **51**, 89 (1963).
⁴P. Filipowicz, J. Javanainen, and P. Meystre, *Phys. Rev. A* **34**, 3077 (1986).
⁵L. Lugiato, M. O. Scully, and H. Walther, *Phys. Rev. A* **36**, 740 (1987).
⁶P. Filipowicz, J. Javanainen, and P. Meystre, *J. Opt. Soc. Am. B* **3**, 906 (1986).
⁷J. Krause, M. O. Scully, and H. Walther, *Phys. Rev. A* **36**,

4547 (1987).

- ⁸P. Meystre, G. Rempe, and H. Walther, *Opt. Lett.* **13**, 1078 (1988).
⁹Theory is described by H. J. Yoo and J. H. Eberly, *Phys. Rep.* **118**, 239 (1985), and references therein.
¹⁰G. Rempe, F. Schmidt-Kaler, and H. Walther, *Phys. Rev. Lett.* **64**, 2783 (1990).
¹¹L. Mandel, *Opt. Lett.* **4**, 205 (1979).
¹²P. Meystre and E. M. Wright, *Phys. Rev. A* **37**, 2524 (1988); P. Meystre, *Opt. Lett.* **12**, 669 (1987).
¹³M. C. Teich and B. E. A. Saleh, *Opt. Lett.* **7**, 365 (1982).